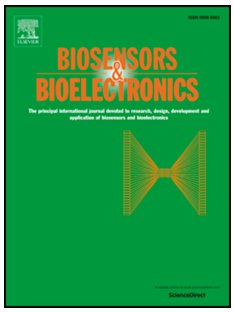

Controlling dopamine binding by the new aptamer for a FRET-based biosensor

Xixia Liu, Yaoyao Hou, Sirui Chen, Juewen Liu

PII: S0956-5663(20)30785-5

DOI: https://doi.org/10.1016/j.bios.2020.112798

Reference: BIOS 112798

To appear in: *Biosensors and Bioelectronics*

Received Date: 9 September 2020

Revised Date: 19 October 2020

Accepted Date: 2 November 2020

Please cite this article as: Liu, X., Hou, Y., Chen, S., Liu, J., Controlling dopamine binding by the new aptamer for a FRET-based biosensor, *Biosensors and Bioelectronics* (2020), doi: https://doi.org/10.1016/j.bios.2020.112798.

Controlling dopamine binding by the new aptamer for a FRET-based biosensor

Xixia Liu[1,2], Yaoyao Hou[1], Sirui Chen[1], Juewen Liu[2]*

[1] Hubei Key Laboratory of Edible Wild Plants Conservation and Utilization, Hubei Normal University, Huangshi, Hubei province, 435002, China

[2] Department of Chemistry, and Waterloo Institute for Nanotechnology, University of Waterloo, Waterloo, ON, N2L 3G1, Canada

Email: liujw@uwaterloo.ca

Abstract:

Dopamine is one of the most important neurotransmitters. A high-quality DNA aptamer for dopamine was reported in 2018. However, fundamental understanding of its binding and folding is lacking, which is critical for related biosensor design. Herein, we performed careful assays using a label-free technique called isothermal titration calorimetry (ITC) to study its secondary structure. We divided this aptamer into four regions and individually examined each of them. We confirmed two stems, but the third stem is believed to be part of a loop. The aptamer was then truncated. The original aptamer had a K_d of 2.2±0.3 μM at 25°C. Shortening the structure by one or two base pairs increased the K_d to 6.9 and 44.4 μM, respectively. Dopamine binding was promoted by both increasing the Mg^{2+} concentration and decreasing the temperature. At 5°C, a K_d of 0.4 μM was achieved. Based on this understanding, we designed two fluorescence resonance energy transfer (FRET) quenching biosensors that differ only by a base pair. The shorter sensor had 3-fold higher sensitivity and a detection limit of 0.9 μM. In 1% fetal bovine serum, the sensor retained a similar limit of detection of 1.14 μM. A two-fluorophore ratiometric FRET sensor was also demonstrated with a low detection limit of 0.12 μM. This work indicated the feasibility of designing folding-based sensors for dopamine, and this design can be extended to other sensing modalities such as electrochemistry and colorimetry.

Keywords: Aptamers, mutation, isothermal titration calorimetry, dopamine, fluorescence resonance energy transfer

Introduction

Dopamine (DA) is a highly important neurotransmitter. In situ measurement of dopamine with a high temporal and spatial resolution is needed to understand related physiological and neurological responses upon stimulation (Benes 2001; Carlsson et al. 1957). Although suffered from interference by other molecules such as uric acid and ascorbate with similar responses, electrochemical sensors based on the redox property of dopamine are the most popular choice (Dandekar and Hentze 1995; Kamal Eddin and Wing Fen 2020; Liu and Liu 2020; Sajid et al. 2016; Tavakolian-Ardakani et al. 2019). To achieve higher specificity, biological ligands for dopamine were also developed. Due to the desire of in situ detection, antibodies are less useful since a quick signal change cannot be easily obtained (Namkung et al. 2017). In this regard, aptamers are more attractive for the selective detection of dopamine.

Aptamers are single-stranded oligonucleotides that can specifically bind target molecules, and are particularly useful for recognizing small molecules (Alkhamis et al. 2019; Gu et al. 2015; Pang et al. 2018; Ruscito and DeRosa 2016; Tabunag et al. 2019; Zhu et al. 2020). Many aptamers, known as riboswitches, were found in the untranslated regions of mRNA to regulate gene expression in bacterial cells and they all bind small molecules or ions (Gilbert and Batey 2005; Jang et al. 2017). An adaptive conformational change is often observed upon an aptamer binding to its target, which makes it easy to design biosensors with specific and fast responses in complex biological environments. An RNA aptamer for dopamine was isolated by Mannironi et al. in 1997 showing a K_d of 1.6 µM (Mannironi et al. 1997). Later, it was reported that the same sequenced DNA could also bind dopamine with an even higher affinity (K_d 0.7 µM) (Walsh and DeRosa 2009). This DNA aptamer has since been widely used to detect dopamine by many research groups (Chen et al. 2019; Huang et al. 2016; Wang et al. 2020; Wei et al. 2019), although some studies raised a concern that it cannot specifically bind dopamine (Álvarez-Martos and Ferapontova 2017).

Recently, direct selection of a DNA aptamer for dopamine was performed by the Stojanović group. This new aptamer (named DA-5bp or the wild-type aptamer in our current work) had a high affinity for dopamine (K_d 0.25 µM based on an indirect fluorescence-based method) (Nakatsuka et al. 2018). Using isothermal titration calorimetry (ITC), we recently reported a K_d of 1.9 µM for this aptamer (Liu et al. 2020). This new aptamer has excellent specificity, whereas its binding of norepinephrine was about 9-fold weaker and tyramine showed no binding at all. Given the excellent performance of this new aptamer, important questions regarding its binding properties have yet to be answered. For example, we wish to know the

critical nucleotides responsible for binding and the conformational change during binding. Such information is useful for designing fold-based biosensors by labeling fluorophore pairs or probes such as 2-aminopurine.

So far, few works have used this aptamer for detecting dopamine. Aside from the original paper using field effect transistors and structure-switching fluorescence detection (Nakatsuka et al. 2018), it was also used for making lateral flow based sensor strips (Dalirirad and Steckl 2020). Its split aptamer was used to develop flexible organic electrochemical transistors (Liang et al. 2020) and logic gate operations (Guo et al. 2020). Aptamer binding often leads to a major conformational change and decreased end-to-end distance, which can be probed using fluorescence resonance energy transfer (FRET) (Dos Santos et al. 2020; Weng et al. 2020; Zhang et al. 2019). This type of folding-based sensor is simple, fast responding, and reversible. FRET has been used for detecting many targets such as platelet-derived growth factor (Yang et al. 2005), potassium (Ueyama et al. 2002) , mercury (Ono and Togashi 2004), and cocaine (Stojanovic et al. 2001). In this work, we first studied dopamine binding and aptamer folding by ITC. Based on our ITC results, we designed FRET-based sensors for dopamine detection, taking advantage of the folding of the aptamer.

Materials and Methods

Chemicals. Dopamine was purchased from sigma-Aldrich (Oakville, ON, Canada). Norepinephrine (NE), ascorbic acid (AA), tyramine (Tyr), glucose (Glu), serotonin (Ser), DL-phenylalanine (Phe), L-dopa (Dopa), and 3,4-dihydroxyphenylacetic acid (DE) were purchased from Aladdin (Shanghai, China). All non-labeled DNA aptamers were synthesized by Integrated DNA Technologies (Coralville, IA, USA). The labeled aptamers were synthesized by Sangon Biotech Ltd. (Shanghai, China). The DNA sequences are shown in Table S1. Salts were purchased from Mandel Scientific (Guelph, ON, Canada) and Sinopharm Chemical Reagent Co., Ltd. (Shanghai, China). Milli-Q water was used for all the experiments to prepare buffers and solutions.

Isothermal Titration Calorimetry (ITC). ITC was performed using a VP-ITC microcalorimeter instrument (MicroCal). Prior to each measurement, all of the solutions were degassed for 5 min to avoid air bubbles. DNA (10 µM, 1.45 mL) in buffer (2.68 mM KCl, 1.46 mM KH_2PO_4, 137 mM NaCl, 8 mM $Na_2HPO_4{\cdot}7H_2O$, 2 mM $MgCl_2$, pH 7.4) was loaded in the ITC cell. Dopamine (0.5 mM, 280 µL) in the same buffer was titrated (10 µL each time) into the cell through a syringe,

except for the first injection (2 µL). The enthalpy (Δ*H*) and association constant K_a were obtained by fitting the titration curves to a one-site binding model using the Origin software. In addition, we tested the temperature (5°C, 15°C, 25°C) and concentration of Mg^{2+} (0, 2 mM, 10 mM) for the wild-type aptamer.

FRET biosensor assay. 10 µL FQ-DA-3bp or FQ-DA-4bp (1 µM) and 40 µL PBS with 2 mM $MgCl_2$ were incubated with 50 µL of dopamine of a series of concentrations (0 µM to 2 mM) for 30 min at room temperature. The fluorescence emission spectra from 500 nm to 650 nm were scanned by excitation at 475 nm using an i3X instrument (Molecular Device, CA, USA). To evaluate the selectivity of the biosensor, 100 nM FQ-DA-3bp was incubated with 50 µM dopamine or its analogs (NE, AA, Tyr, Glu, Ser, Phe, L-dopa, DE) for 30 min at room temperature. The fluorescence intensity at 520 nm were recorded with excitation at 475 nm. To follow the kinetics of sensor response, the background fluorescence of 10 µL FQ-DA-3bp (1 µM) and 88 µL PBS with 2 mM $MgCl_2$ was monitored for 5 min with excitation at 475 nm and emission at 520 nm. Then 2 µL dopamine was added and the fluorescence was monitored for another 10 min. For the assay with FR-DA-3bp, the operations were the same with 475 nm excitation. The ratio of the two peaks at 580 nm and 520 nm was plotted for the calibration curve.

Dopamine detection in 1% fetal bovine serum (FBS). The background fluorescence of 1% FBS was first measured. Then, the fluorescence intensities of different samples (100 nM FQ-DA-3bp, 100 nM FQ-DA-3bp + 50 µM dopamine, buffer, and dopamine) in 1% FBS were measured after incubation for 30 min with excitation at 475 nm.

Results and Discussion

Mutation to understanding the critical nucleotides and secondary structure

The predicted secondary structure of the aptamer is shown in Figure 1A. It has a small stem loop (region 1), a large loop (region 2), a mismatched base pair region (3) and a 5-base-pair stem to close the structure (region 4). Our first goal is to understand this secondary structure by making some simple mutations. To measure dopamine binding, we used ITC, which directly measures the heat of the binding reaction allowing the extraction of thermodynamic constants. Since no covalent labels or other probes were needed, it is a reliable method (Amano et al. 2019; Neves et al. 2017; Oni et al. 2017; Slavkovic and Johnson 2018).

The wild-type aptamer (named DA-5bp since it has 5 base pairs in the stem) had a large amount of heat released with a K_d of 2.2±0.3 μM. Since regions 1 and 4 have fully base paired stems, their structures are likely to be reliable. However, region 3 has two mismatches and whether the rest nucleotides can base pair or not is questionable. Region 3 has two A-T base pairs. If their roles are only to form base pairs, an A-T pair should be changeable to a T-A pair and *vice versa*. We then tested the top T-A base and the mutant was named DA-mut1 (Figure 1A). However, the binding activity was fully abolished (Figure 2B), suggesting that this T-A is actually not a base pair. Since the base pair above it is a less stable G-T wobble, we reason that these two base pairs cannot form. Similarly, we switched the lower A-T pair to T-A (named DA-mut2), and the binding was lost as well (Figure 2C). In addition, we fixed the C-A mismatch to make it a T-A base pair (DA-mut3). Interestingly, this mutant had a K_d of 2.3±0.5 μM (Figure 2D), similar to the wild-type aptamer. Therefore, this C-A should be base paired and thus not involved in dopamine binding. Therefore, region 2 and part of region 3 form a larger loop for dopamine binding as shown in Figure 1B.

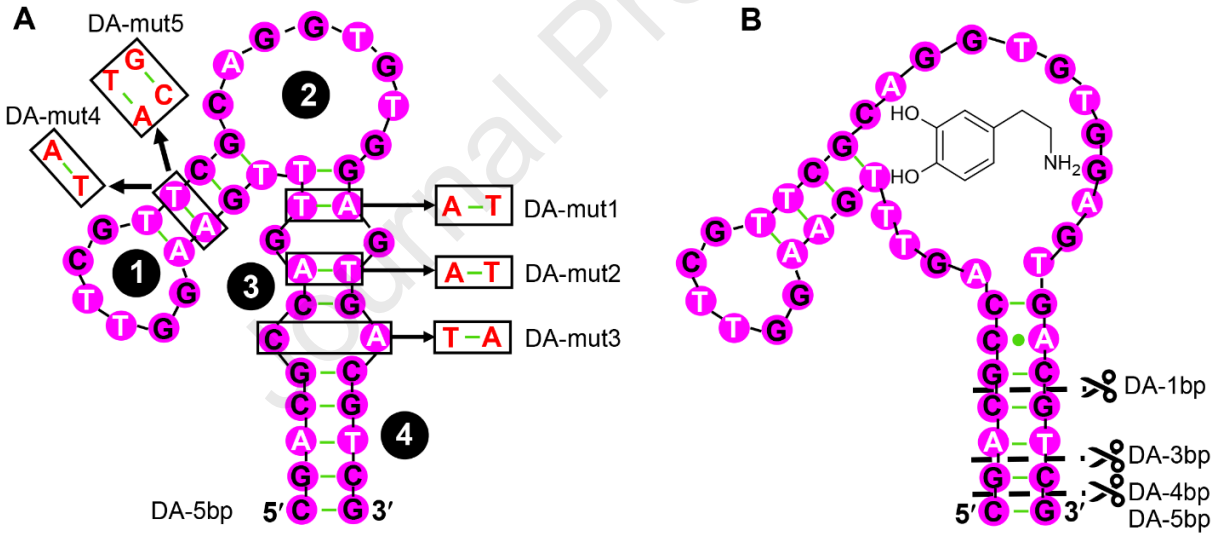

Figure 1. (A) The predicted secondary of the originally reported wild-type aptamer named DA-5bp and some mutants designed to test this secondary structure. The structure is divided into four regions. (B) The secondary structure of the aptamer based on the mutation study, and some further truncation of the aptamer is also shown.

Finally, we tested region 1 and switched one of the T-A base pairs to A-T (DA-mut4).The K_d of this mutant was 2.8±0.8 μM (Figure 2E). Therefore, the stem in region 1 is indeed a stem.

We further extended the length of the stem of region 1 by an extra G-C pair (DA-mut5), and the binding was fully abolished (Figure 2F). Therefore, it is likely that this stem connects the two loops in region 1 and 2 to afford dopamine binding. These mutation studies have refined the secondary structure of the aptamer (Figure 1B). The thermodynamic parameters of these binding reactions are listed in Table S2.

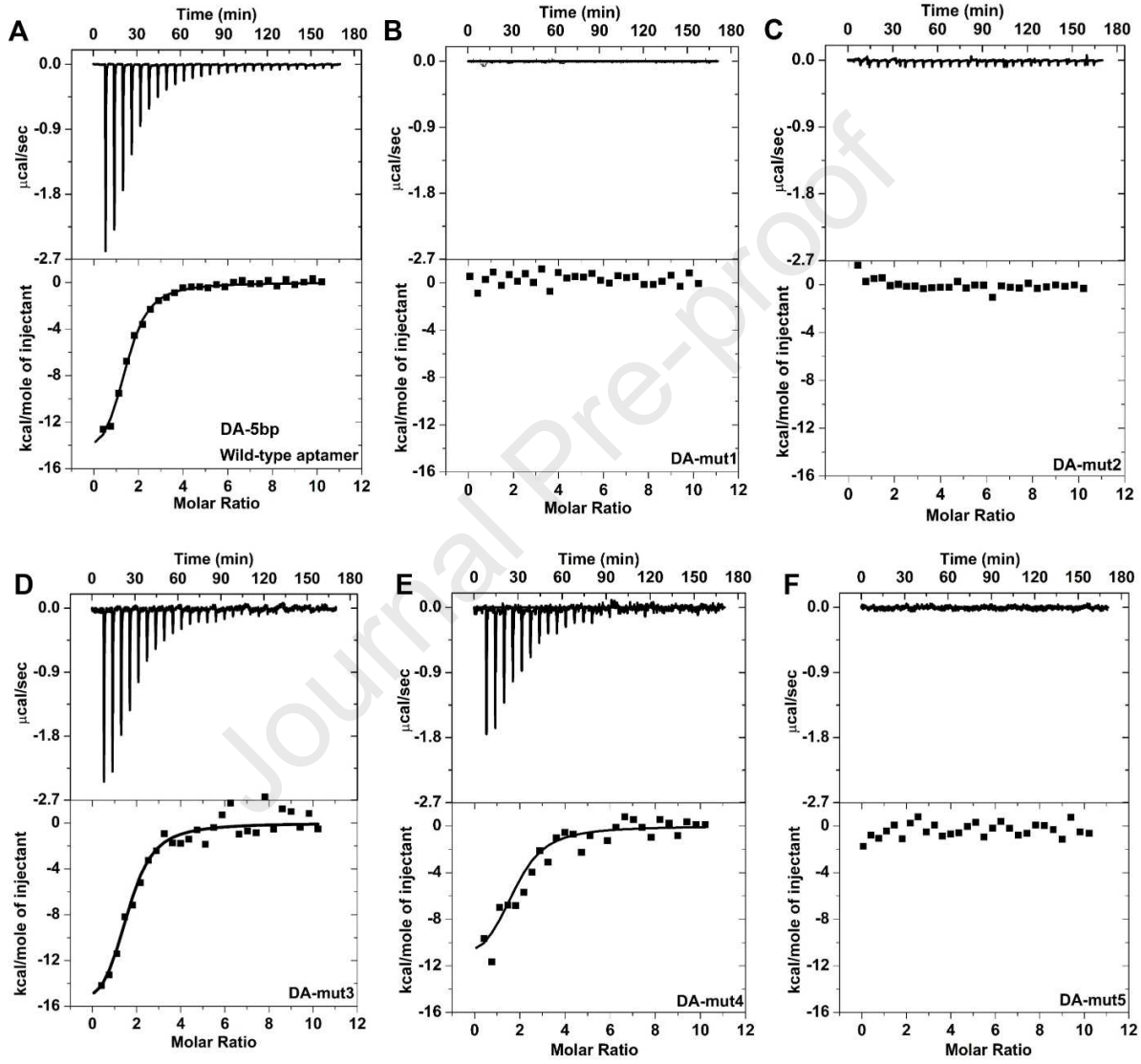

Figure 2. ITC analysis of the aptamer mutants. ITC traces of titrating 0.5 mM dopamine into 10 µM (A) the wild-type aptamer DA-5bp, (B) DA-mut1, (C) DA-mut2, (D) DA-mut3, (E) DA-mut4, (F) DA-mut5. The dopamine and aptamer were dissolved in PBS with 2 mM $MgCl_2$ (pH 7.4).

Truncation of the aptamer

A goal of this work is to develop a folding-based aptamer sensor. For this purpose, it is important to have an open state for the aptamer before binding to the target and then a closed state after binding. The current aptamer has five base pairs at the ends. We wondered if this stem can be shortened. We gradually truncated 1 base pair (DA-4bp), 2 base pairs (DA-3bp), and 4 base pairs (DA-1bp) (see Figure 1B). Their ITC results are shown in Figure 3. For DA-4bp (Figure 3A), the K_d was 6.9 μM, which increased about 3-fold compared to the wild-type. For DA-3bp (Figure 3B), the K_d drastically increased to 44 μM, and the amount of heat released was significantly decreased. For DA-1bp (Figure 3C), no measurable binding was detected. These truncated aptamers indicated that a stable stem in region 4 is critical for high affinity binding of dopamine, and truncation would lead to a lower binding affinity. However, when this stem is too long, the stem might be closed even before binding of dopamine, disallowing FRET-based sensing.

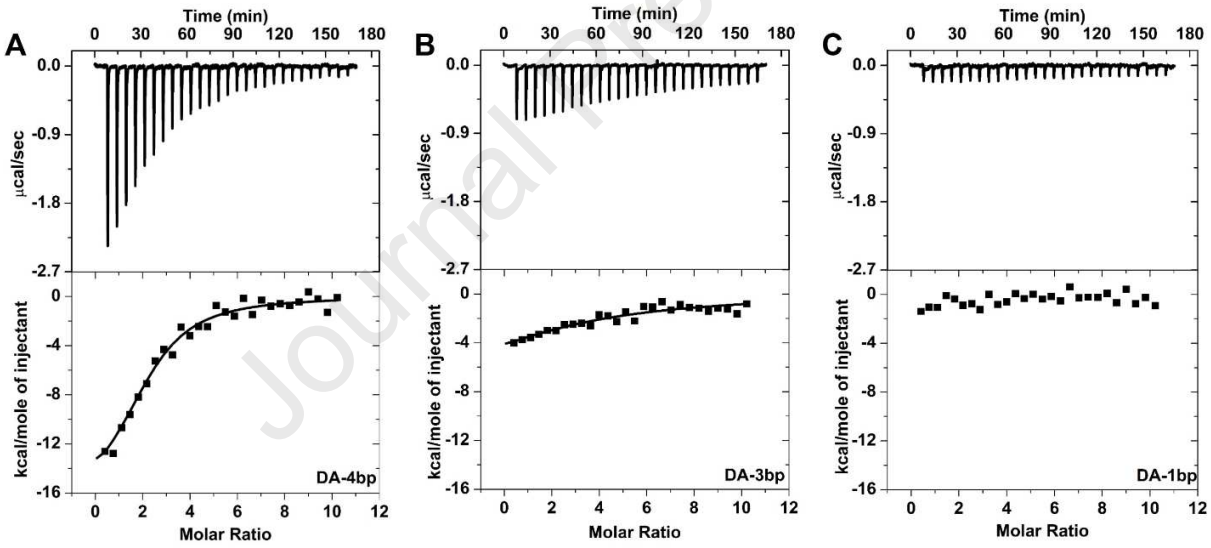

Figure 3. ITC analysis of the truncated aptamers. ITC traces of titrating 0.5 mM dopamine into 10 μM (A) DA-4bp, (B) DA-3bp, and (C) DA-1bp. The dopamine and aptamer were dissolved in PBS with 2 mM $MgCl_2$ (pH 7.4).

Effect of salt and temperature.

To further understand dopamine binding, we tested the effect of temperature (Figure 4A-C) Detailed binding information is shown in Table 1. At 5°C, the binding became very tight and

reached a K_d of 0.35 μM. It is interesting to note that the released heat decreased and the entropy loss due to the binding dropped significantly. Therefore, the tighter binding at 5°C was mainly driven by the entropic factor. We reason that the aptamer already formed a well-folded structure at low temperatures and the binding occurred without a major structural change (e.g. lock-and-key).

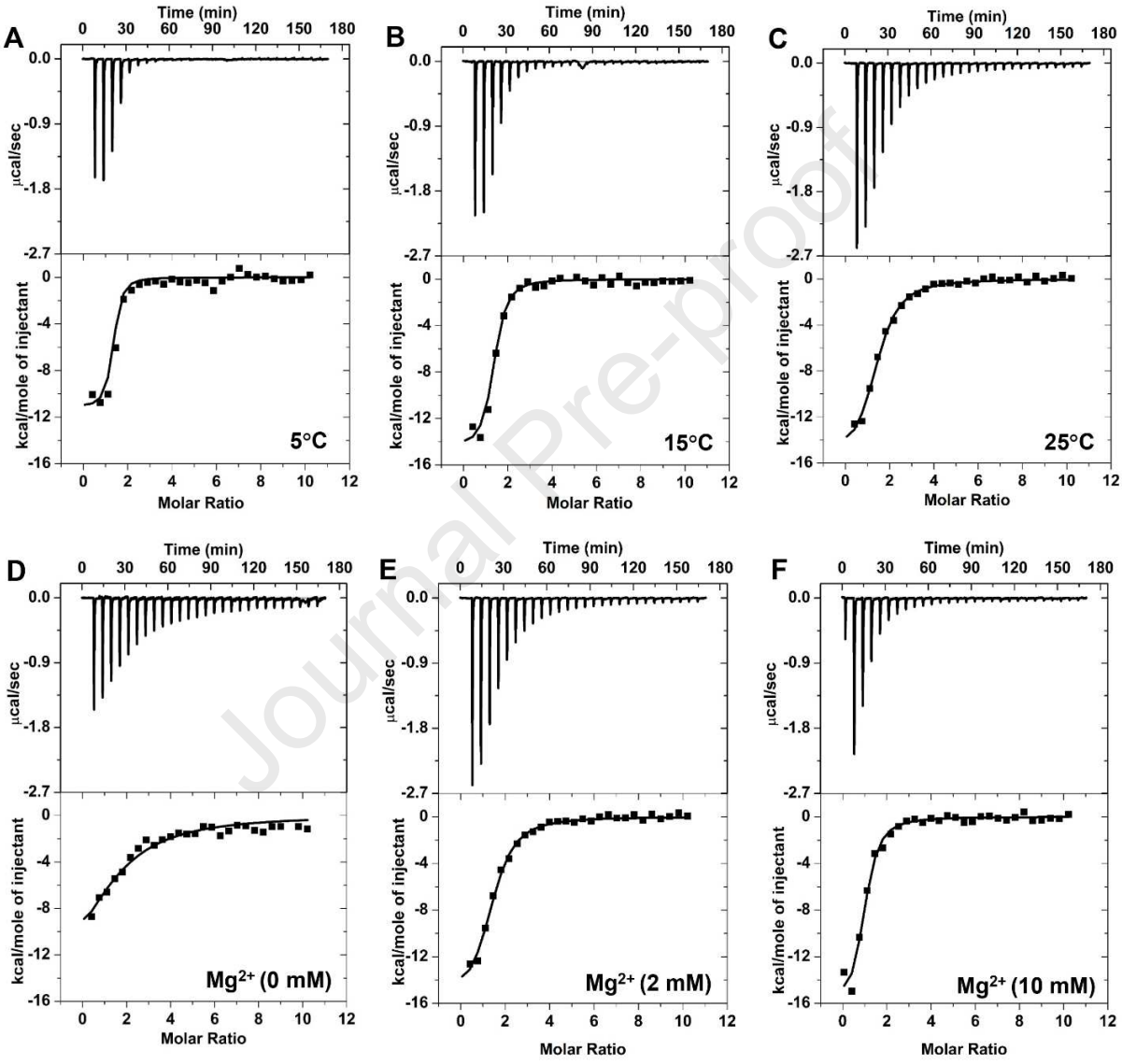

Figure 4. ITC traces of titrating 0.5 mM dopamine into 10 μM wild-type aptamer DA-5bp at different temperatures: (A) 5°C, (B) 15°C, (C) 25°C. ITC traces of titrating 0.5 mM dopamine into 10 μM DA-5bp at different concentrations of Mg^{2+}: (D) 0 mM, (E) 2 mM, (F) 10 mM.

We then studied the effect of salt concentration (Figure 4D-F), which is critical for biosensing applications. Our normal buffer was PBS with 2 mM Mg^{2+} and the K_d was ~2.2 µM. In the PBS buffer without Mg^{2+}, the K_d became 17.2 µM. With 10 mM Mg^{2+}, the binding was slightly tighter with a K_d of 1.3 µM. Therefore, Mg^{2+} could promote aptamer binding and 2 mM Mg^{2+} was close to saturation. Careful observation of the thermodynamic values revealed a similar trend as the temperature changed (Table 1). This information is useful for sensor design, since a large conformational change can be used to develop a FRET-based sensor probing the end-to-end distance change.

Table 1. Thermodynamic binding values of the wild-type aptamer at different temperature and concentration of Mg^{2+}.

		N	K_a ($\times 10^6$ M^{-1})	K_d (µM)	Δ*H* (kcal M^{-1})	Δ*S* (cal K^{-1} M^{-1})
Temperature	5	1.2±0.1	3.6±1.9	0.4±0.2	-12.1±0.7	-9.7±0.8
(°C)	15	1.3±0.1	1.5±0.4	0.7±0.2	-14.7±0.6	-21.6±1.3
	25	1.2±0.1	0.5±0.1	2.2±0.3	-15.9±0.6	-29.5±2.8
[Mg^{2+}]	0	1.4±0.3	0.06±0.02	17.2±5.8	-18.3±6.3	-43.7±5.7
(mM)	2	1.2±0.1	0.5±0.1	2.2±0.3	-15.9±0.6	-29.5±2.8
	10	0.9±0.1	0.8±0.2	1.3±0.1	-16.7±0.9	-28.8±0.6

Notes: Data obtained using a one-site binding model.

FRET based quenching biosensors

This new aptamer has not yet been widely used for biosensor development. In the original selection paper, a structure-switching sensor was reported using two DNA strands (Nakatsuka et al. 2018). This sensor was highly sensitive but since it had two DNA strands, it may not be reversible due to the time needed to hybridize the strands in dilute conditions (Nutiu and Li 2003, 2004). In this work, we first designed a reversible sensor by labeling a fluorophore and a quencher on the two ends as shown in Figure 5A. In the presence of dopamine, the two ends come together resulting in fluorescence quenching. For this method to work, the DNA needs to

be initially in an open state. However, the original aptamer sequence has 5 base pairs in the stem region and is likely to be already in the closed state. Our ITC measurement above using different stem lengths indicated that the binding still occurred when the stem length was shortened, even though the binding affinity decreased. Based on this understanding, we designed two sensor sequences by deleting one or two base pairs in the stem region (named FQ-DA-4bp and FQ-DA-3bp). For each sensor DNA, a FAM fluorophore was labeled on the 5′-end and a dark quencher was labeled on the 3′-end.

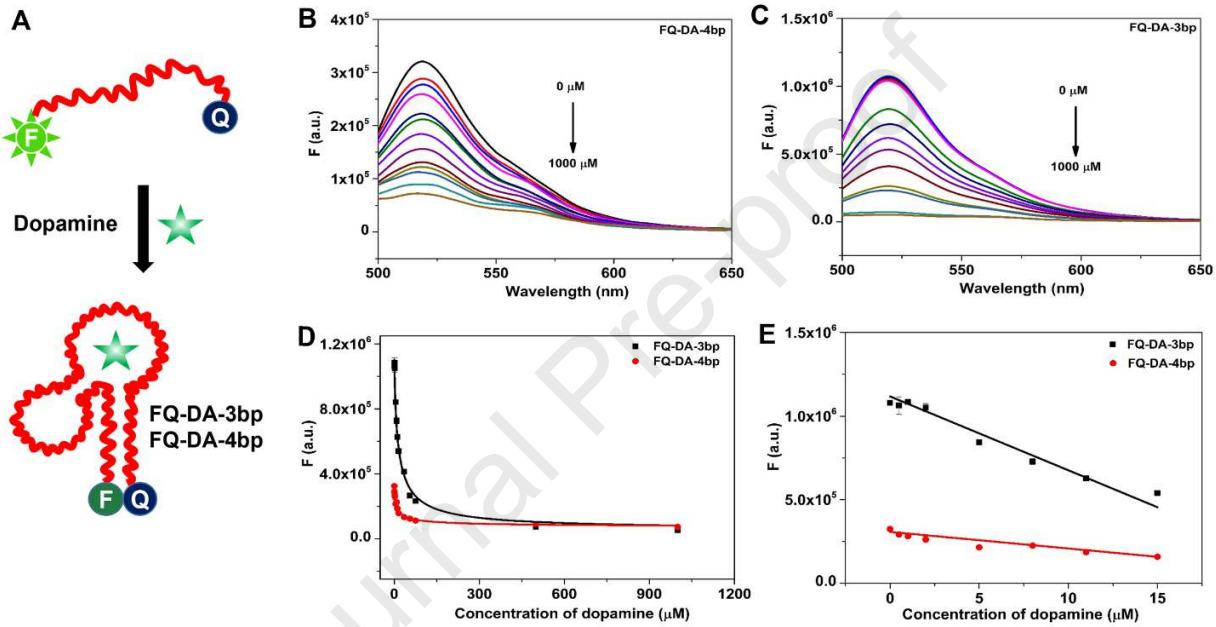

Figure 5. (A) A scheme of the FRET-based sensor with 3 or 4 base pairs in the stem region. The fluorescence spectra of (B) FQ-DA-4bp and (C) FQ-DA-3bp incubated with various concentrations of dopamine. Note that the *y*-axis scales are different for them. (D) The binding curves of these two sensors. (E) The initial linear relationship of the fluorescence intensity of the two sensors at low concentrations of dopamine. The dopamine and DNA were dissolved in PBS with 2 mM $MgCl_2$ (pH 7.4).

Using the same sensor concentration, we performed a dopamine titration experiment. In both sensors, we indeed observed dopamine concentration-dependent fluorescence quenching (Figure 5B, C). Before adding dopamine, the FQ-DA-4bp sensor had a much lower initial fluorescence suggesting that this DNA was mostly already in the closed hairpin state. Both sensors showed a nice binding curve with the K_d fitted to be 8 and 14 μM, respectively.

Therefore, although the FQ-DA-3bp sensor had a larger signal change, its binding to the target was weaker due to a less stable stem. By fitting the initial fluorescence drop in up to 15 µM dopamine, a linear response was observed for both sensors. The FQ-DA-3bp sensor had a 4.5-fold higher sensitivity based on the measurement of the slope. Therefore, the FQ-DA-3bp sensor was used for subsequent studies, and we determined its detection limit to be 0.9 µM dopamine based on the signal greater than three times of background variation. It needs to be pointed out that for real applications, other compounds such as proteins and salts, temperature and crowded cellular or other biological environment might also affect the performance of the sensor. The sensor design might need to be optimized to fit the actual analytical sample matrix and environment.

Characterization and application of the FQ-DA-3bp sensor.

Using the FQ-DA-3bp sensor, we then followed the kinetics of the fluorescence change (Figure 6A). The fluorescence intensity rapidly decreased when dopamine was added, indicating the aptamer immediately closed when bound with dopamine and this system can quickly reach equilibrium. This feature makes this aptamer valuable for in situ measurement with a high temporal resolution. We also measured the selectivity in the presence of dopamine and its various analogs (Figure 6B). When 50 µM dopamine was added, the fluorescence had an obvious drop of ~70%. The next change was observed with norepinephrine at 25%, which was consistent with its weaker binding to the aptamer (Nakatsuka et al. 2018). Further improvement in specificity might be achieved by doing more stringent counter selections should the binding of norepinephrine be a concern. Little changes were observed in the present of its other analogs, indicating the sensor had high specificity to detect dopamine.

To test the performance of the sensor in real samples, we used 1% fetus bovine serum (FBS). With our excitation wavelength of 475 nm, neither free dopamine nor 1% FBS had a strong background fluorescence to interfere with the sensor (Figure 6C). The expected fluorescence quenching induced by dopamine was also observed (Figure 6C). We further performed a titration of dopamine in 1% FBS (Figure 6D). The K_d was 13.6 µM and the linear range was from 0 µM to 15 µM with LOD of 1.14 µM. These data were similar to that in the clean buffer, indicating the sensor was robust and can be potentially used for detection in real samples.

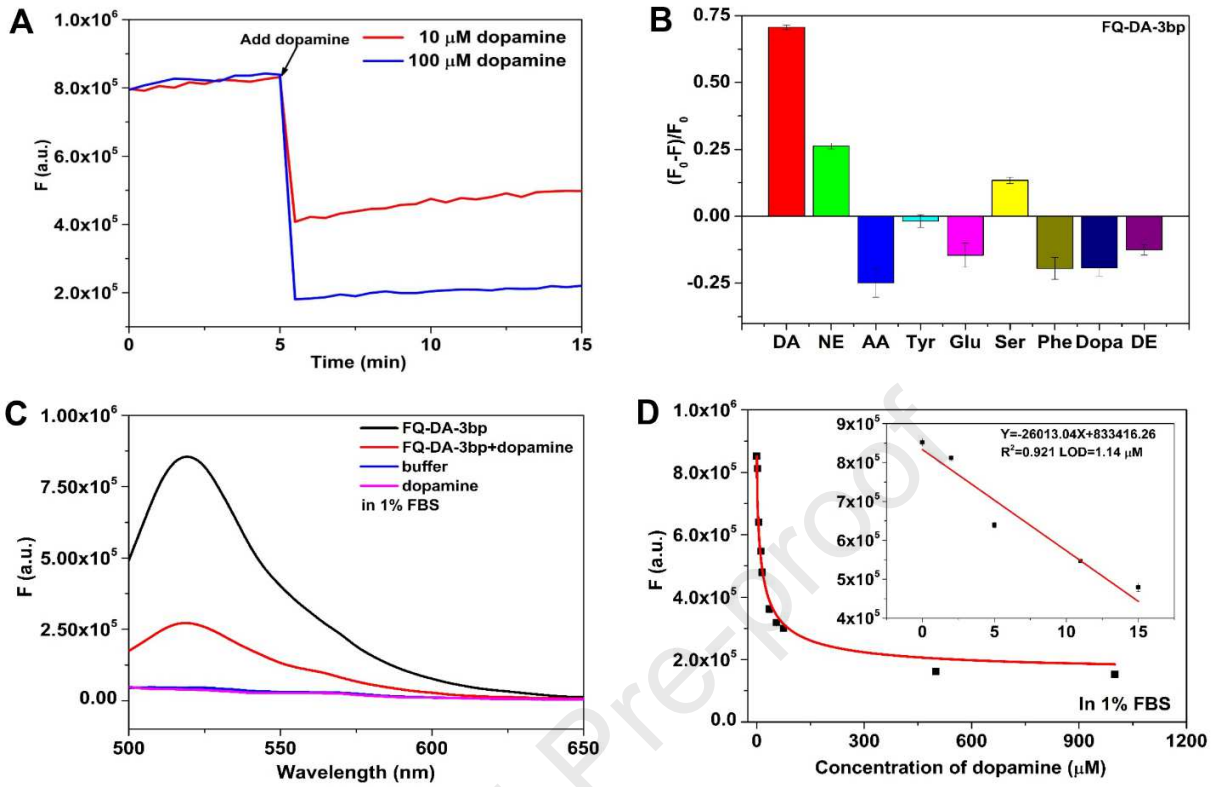

Figure 6. (A) The kinetics of the fluorescence change upon the addition of dopamine. (B) The selectivity of the FQ-DA-3bp sensor with 50 μM analytes. DA: dopamine; NE: norepinephrine; AA: ascorbic acid; Tyr: tyramine; Glu: glucose; Ser: serotonin; Phe: DL-phenylalanine; Dopa: L-dopa; DE: 3,4-dihydroxyphenylacetic acid. (C) The fluorescence spectra of the 100 nM DQ-DA-3bp incubated with 50 μM dopamine in 1% FBS (diluted in PBS with 2 mM Mg^{2+}). (D) 100 nM FQ-DA-3bp sensor response to various concentrations of dopamine in 1% FBS.

A FRET based ratiometric biosensor

Finally, we replaced the quencher by another fluorophore, tetramethylrhodamine (TAMRA) as shown in Figure 7A (Ueyama et al. 2002; Urata et al. 2007). TAMRA has an emission peak at 580 nm. Upon binding dopamine, the distance between the FAM and TAMRA labels became shorter. Upon excitation of FAM, the relative emission of TAMRA was expected to increase. Such a design would allow ratiometric detection. Indeed as shown in Figure 7B, when excited at 475 nm, the relatively increased 580 nm peak was observed. We plotted the ratio of these two peaks (Figure 7C) and based on it, a detection limit of 0.12 μM dopamine was obtained, which was 7-fold lower than of the quenching-based sensor.

Many sensing methods have been reported for detecting dopamine, such as those based on various enzymes, antibodies and electrochemistry. Aptamer-based sensors can have a rapid and large conformational change, which is desirable to fight against nonspecific binding in biological samples (Lubin and Plaxco 2010). Most previous sensors used the other DNA aptamer derived from an RNA aptamer. Some sensors using the new aptamer are listed in Table S3. Our sensors had comparable sensitivity with many other sensors, but are simpler and immobilization free.

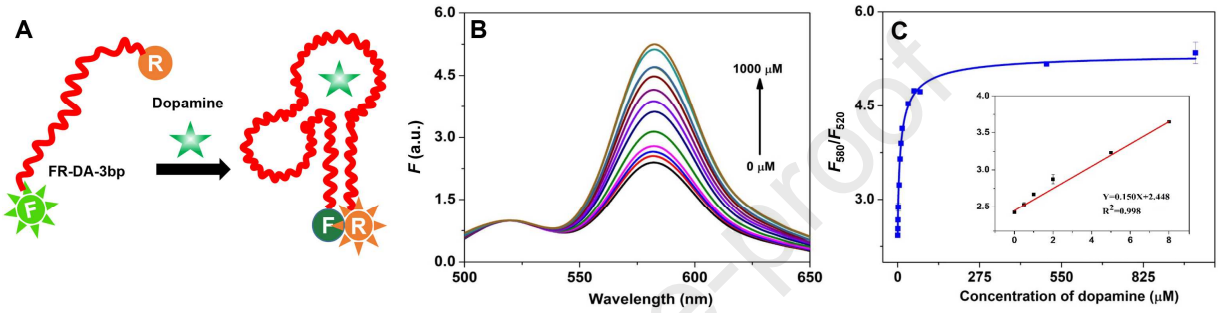

Figure 7. (A) A scheme of FRET-based dopamine detection by labeling the DA-3bp aptamer by FAM and TAMRA at the two ends, and this DNA is named FR-DA-3bp. (B) Normalized fluorescence spectra of the sensors in the presence of different concentrations of dopamine. (C) The FR-DA-3bp sensor response to various concentrations of dopamine. Inset: the linear response at low dopamine concentrations.

Conclusions

In summary, we have systematically studied the binding characteristics of a newly selected aptamer for dopamine. We designed mutants to test its secondary structure and revealed important new base pairs that refined the previously predicted structure. By truncating the stem region, we obtained the minimal binding sequence. The effects of temperature and Mg^{2+} concentration on binding were also measured using ITC. This knowledge enabled us to design FRET-based sensors to detect dopamine in buffer and in FBS with a fast response. Two sensor DNA sequences were designed and differ by only a single base pair. The longer sensor had lower initial fluorescence and thus less signal change. While the shorter sensor had more signal change, its binding affinity was lower. Finally, a FRET-based ratiometric sensor was also demonstrated with a low detection limit of 0.27 μM dopamine. This study has answered important questions regarding this DA-5bp aptamer. The binding induced folding of the aptamer

can be used for designing other sensors based on electrochemistry or colorimetry for dopamine detection.

Acknowledgement

Funding for this work was from the Natural Sciences and Engineering Research Council of Canada (NSERC), and the National Natural Science Foundation of China (31601548). X. Liu was supported by a China Scholarship Council (CSC) Scholarship, and Hubei Youth Science and Technology Morning-light Program (No. 2019) to visit the University of Waterloo.

Appendix A. Supplementary data

Supplementary data to this article can be found in supplementary information

References

Alkhamis, O., Canoura, J., Yu, H.X., Liu, Y.Z., Xiao, Y., 2019. Trac-Trends Anal. Chem. 121, 115699.

Álvarez-Martos, I., Ferapontova, E.E., 2017. Biochem. Biophys. Res. Commun. 489, 381-385.

Amano, R., Furukawa, T., Sakamoto, T., 2019. ITC Measurement for High-Affinity Aptamers Binding to Their Target Proteins. In: Ennifar, E. (Ed.), Microcalorimetry of Biological Molecules: Methods and Protocols, pp. 119-128. Springer New York, New York, NY.

Benes, F.M., 2001. Trends Pharmacol. Sci. 22, 46-47.

Carlsson, A., Lindqvist, M., Magnusson, T., 1957. Nature 180, 1200-1200.

Chen, J., Li, Y.C., Huang, Y.N., Zhang, H.J., Chen, X.G., Qiu, H.D., 2019. Microchimica Acta 186.

Dalirirad, S., Steckl, A.J., 2020. Anal. Biochem. 596, 113637-113637.

Dandekar, T., Hentze, M.W., 1995. Trends Genet. 11, 45-50.

Dos Santos, M.C., Algar, W.R., Medintz, I.L., Hildebrandt, N., 2020. Trac-Trends Anal. Chem. 125, 115819.

Gilbert, S.D., Batey, R.T., 2005. Cell. Mol. Life Sci. 62, 2401-2404.

Gu, C., Lan, T., Shi, H., Lu, Y., 2015. Anal. Chem. 87, 7676-7682.

Guo, T., Wu, C.T., Offenhaeusser, A., Mayer, D., 2020. Physica Status Solidi A 217, 1900924.

Huang, H.L., Shi, S., Gao, X., Gao, R.R., Zhu, Y., Wu, X.W., Zang, R.M., Yao, T.M., 2016. Biosens. Bioelectron. 79, 198-204.

Jang, S., Jang, S., Xiu, Y., Kang, T.J., Lee, S.H., Koffas, M.A.G., Jung, G.Y., 2017. ACS Synth. Biol. 6, 2077-2085.

Kamal Eddin, F.B., Wing Fen, Y., 2020. Sensors 20, 1039.

Liang, Y.Y., Guo, T., Zhou, L., Offenhausser, A., Mayer, D., 2020. Materials 13, 2577.

Liu, X., He, F., Zhang, F., Zhang, Z., Huang, Z., Liu, J., 2020. Anal. Chem. 92, 9370–9378.

Liu, X., Liu, J., 2020. VIEW, DOI: 10.1002/VIW.20200102.

Lubin, A.A., Plaxco, K.W., 2010. Acc. Chem. Res. 43, 496-505.

Mannironi, C., Di Nardo, A., Fruscoloni, P., Tocchini-Valentini, G.P., 1997. Biochemistry 36, 9726-9734.

Nakatsuka, N., Yang, K.-A., Abendroth, J.M., Cheung, K.M., Xu, X., Yang, H., Zhao, C., Zhu, B., Rim, Y.S., Yang, Y., Weiss, P.S., Stojanović, M.N., Andrews, A.M., 2018. Science 362, 319-324.

Namkung, S., Choi, J.S., Hyang, P.J., Yang, M.-G., Lee, M.W., Kim, S.W., 2017. Korean J. Clinical Lab. Sci. 49, 220-226.

Neves, M.A.D., Shoara, A.A., Reinstein, O., Abbasi Borhani, O., Martin, T.R., Johnson, P.E., 2017. ACS Sensors 2, 1539-1545.

Nutiu, R., Li, Y., 2003. J. Am. Chem. Soc. 125, 4771-4778.

Nutiu, R., Li, Y., 2004. Chem. Eur. J. 10, 1868-1876.

Oni, O., Zhang, Z., Liu, J., 2017. Nucleic Acids Res. 45, 7593-7601.

Ono, A., Togashi, H., 2004. Angew. Chem. Int. Ed. 43, 4300-4302.

Pang, X.H., Cui, C., Wan, S., Jiang, Y., Zhang, L.L., Xia, L., Li, L., Li, X.W., Tan, W.H., 2018. Cancers 10, 47.

Ruscito, A., DeRosa, M.C., 2016. Front. Chem. 4, 14.

Sajid, M., Nazal, M.K., Mansha, M., Alsharaa, A., Jillani, S.M.S., Basheer, C., 2016. TrAC-Trends Anal. Chem. 76, 15-29.

Slavkovic, S., Johnson, P.E., 2018. Aptamers 2, 45-51.

Stojanovic, M.N., de Prada, P., Landry, D.W., 2001. J. Am. Chem. Soc. 123, 4928-4931.

Tabunag, J.S., Guo, Y.J., Yu, H.Z., 2019. J. Anal. Test. 3, 107-116.

Tavakolian-Ardakani, Z., Hosu, O., Cristea, C., Mazloum-Ardakani, M., Marrazza, G., 2019. Sensors 19, 2037.

Ueyama, H., Takagi, M., Takenaka, S., 2002. J. Am. Chem. Soc. 124, 14286-14287.

Urata, H., Nomura, K., Wada, S.-i., Akagi, M., 2007. Biochem. Biophys. Res. Commun. 360, 459-463.

Walsh, R., DeRosa, M.C., 2009. Biochem. Biophys. Res. Commun. 388, 732-735.

Wang, Y., Kang, K., Wang, S., Kang, W., Cheng, C., Niu, L.M., Guo, Z., 2020. Sensor. Actuat. B: Chem. 305, 127348.

Wei, B., Zhong, H., Wang, L., Liu, Y., Xu, Y., Zhang, J., Xu, C., He, L., Wang, H., 2019. Int. J. Biol. Macromol. 135, 400-406.

Weng, C., Fan, N.Q., Xu, T.R., Chen, H.D., Li, Z.F., Li, Y.W., Tan, H., Fu, Q., Ding, M.M., 2020. Chin. Chem. Lett. 31, 1490-1498.

Yang, C.J., Jockusch, S., Vicens, M., Turro, N.J., Tan, W., 2005. Proc. Natl. Acad. Sci. U.S.A. 102, 17278-17283.

Zhang, X.J., Hu, Y., Yang, X.T., Tang, Y.Y., Han, S.Y., Kang, A., Deng, H.S., Chi, Y.M., Zhu, D., Lu, Y., 2019. Biosensor. Bioelectron. 138, 111314.

Zhu, C., Li, L.S., Wang, Z.J., Irfan, M., Qu, F., 2020. Biosensor. Bioelectron. 160, 112213.

- Structure and sequence requirement for the new dopamine aptamer characterized by ITC.
- The buffer and temperature dependent binding of dopamine measured.
- A folding based FRET sensor designed, and this information is useful for developing other types of biosensors using this aptamer.

CRediT author statement

Xixia Liu: Experimentation, Conceptualization, Writing. **Yaoyao Hou**: Experimentation. **Sirui Chen**: Experimentation. **Juewen Liu**: Conceptualization, Writing, Editing.

Declaration of interests

☒ The authors declare that they have no known competing financial interests or personal relationships that could have appeared to influence the work reported in this paper.

☐The authors declare the following financial interests/personal relationships which may be considered as potential competing interests: